

Autophoresis of two adsorbing/desorbing particles in an electrolyte solution

Fan Yang¹, Bhargav Rallabandi^{1,‡} and Howard A. Stone^{1,†}

¹Department of Mechanical and Aerospace Engineering, Princeton University, Princeton, NJ 08544, USA

(Received 22 May 2018; revised 4 January 2019; accepted 12 January 2019)

Classical diffusiophoresis describes the motion of particles in an electrolyte or non-electrolyte solution with an imposed concentration gradient. We investigate the autophoresis of two particles in an electrolyte solution where the concentration gradient is produced by either adsorption or desorption of ions at the particle surfaces. We find that when the sorption fluxes are large, the ion concentration near the particle surfaces, and consequently the Debye length, is strongly modified, resulting in a nonlinear dependence of the phoretic speed on the sorption flux. In particular, we show that the phoretic velocity saturates at a finite value for large desorption fluxes, but depends superlinearly on the flux for adsorption fluxes, where both conclusions are in contrast with previous results that predict a linear relationship between autophoretic velocity and sorption flux. Our theory can also be applied to precipitation/dissolution and other surface chemical processes.

Key words: colloids

1. Introduction

A particle adsorbing or desorbing solutes in an otherwise uniform solution creates a concentration gradient, which may cause the particle to move due to diffusiophoresis. This process, which can occur without applying any external concentration fields, is called ‘autophoresis’ or ‘self-diffusiophoresis’. There are mainly two types of approaches to model this process. The first exploits continuum mechanics by neglecting the finite size of solute molecules (Anderson 1989; Golestanian, Liverpool & Ajdari 2007; Michelin, Lauga & Bartolo 2013; Sharifi-Mood, Koplik & Maldarelli 2013; Michelin & Lauga 2014) and steric effects of solute molecules are only considered when the solute concentration is large (Kilic, Bazant & Ajdari 2007; Bazant *et al.* 2009). The second approach adopts a colloidal perspective by modelling both the particle and solute molecules as interacting colloids (Córdova-Figueroa & Brady 2008; Brady 2011). Results of these two approaches have been found to be the same when the solution is dilute and the size of solute molecules is small (Brady 2011). In this paper, we utilize the continuum approach, which is valid in many

† Email address for correspondence: hastone@princeton.edu

‡ Present address: Department of Mechanical Engineering, University of California, Riverside, CA 92521, USA

experiments on self-propelled colloids (Paxton, Sen & Mallouk 2005; Howse *et al.* 2007; Sen *et al.* 2009; Wang *et al.* 2013; Brown & Poon 2014).

For the common limit of a low-Reynolds-number and low-Péclet-number motion, an isolated sphere with uniform surface reactions in an electrolyte solution will not move due to symmetry. Therefore, symmetry should be broken to establish a preferred direction for translation. This symmetry breaking is usually introduced via either chemical (Mozaffari *et al.* 2016) or geometric asymmetry (Shklyaev, Brady & Córdoba-Figueroa 2014; Michelin & Lauga 2015; Schnitzer & Yariv 2015; Yariv 2016). However, in the moderate-Péclet-number regime, Michelin *et al.* (2013) predicted that an isolated isotropic particle is unstable above a critical Péclet number, resulting in a spontaneous autophoretic motion, which was later verified in experiments (Izri *et al.* 2014). In this paper, we assume both Reynolds and Péclet numbers are small and consider the interactions of two particles.

A chemical asymmetry requires that the chemical properties of a particle are non-uniform, such as occurs for Janus particles, whose surface is non-uniformly covered by active chemicals that can either dissolve into or react with the surrounding solution (Sen *et al.* 2009; Moran & Posner 2011; Mozaffari *et al.* 2016); also, see reviews by Velegol *et al.* (2016), Moran & Posner (2017) and Safdar, Khan & Jänis (2018). Recently Ibrahim, Golestanian & Liverpool (2017) studied the effect of electrokinetics on the self-propulsion of a Janus particle and Tătulea-Codrean & Lauga (2018) calculated the motion of Janus particles in a chemical gradient. On the other hand, a geometric asymmetry is much easier to generate without the need to modify the surface chemical properties (Baraban *et al.* 2012). Typical asymmetric geometries include a sphere in a fluid with nearby boundaries (Yariv 2016), two spheres in an infinite fluid (Michelin & Lauga 2015; Moerman *et al.* 2017) and an asymmetric particle shape (Michelin & Lauga 2015; Schnitzer & Yariv 2015). These theoretical studies all assume a linear relation between the diffusiophoretic slip velocity and the local concentration gradient and, as a consequence, predict a linear increase of the diffusiophoretic particle speed with the ion flux due to sorption at the particle's surface, independent of the local concentration on the particle surface.

In this paper, using a more systematic account of diffusiophoretic mechanisms, we study the autophoresis of two particles with uniform sorption fluxes and show that the results in previous studies only apply to small sorption fluxes. The diffusiophoretic slip velocity not only depends on the concentration gradient, but also on the range over which the intermolecular potential decays. This range is usually related to the local concentration on the particle surface. Therefore, when the sorption flux is large enough to significantly modify the solute concentration and consequently the typical range of the intermolecular potential on the particle surface, the diffusiophoretic slip velocity is no longer independent of the local concentration (Prieve *et al.* 1984). A consequence of this feature is that the autophoretic velocity is not linear in sorption flux. In particular, we find that in electrolyte solutions, for large desorption fluxes, the diffusiophoretic velocity saturates at a finite value, and that for large adsorption fluxes, the velocity grows superlinearly with flux. Both predictions are in contrast with the theoretical results of diffusiophoresis in a non-electrolyte solution reported by Michelin & Lauga (2014) and Yariv (2016). However, these earlier results can be recovered as a limiting case of our analysis for weak sorption fluxes. Furthermore, we argue that the large-flux regime is relevant to many experimental studies of phoretic self-propulsion (Paxton *et al.* 2005; Howse *et al.* 2007), and the dependence of the interaction layer thickness on the local concentration field is qualitatively to be expected for a wide range of surface potentials.

2. Discussion of the slip velocity due to diffusiophoresis

The diffuse layer of solute molecules/ions residing adjacent to a particle surface is the region where the diffusive solute flux due to gradients in chemical concentration balances the flux due to an intermolecular potential ϕ describing short-range interactions between the particle and solute molecules/ions. The thickness of the diffuse layer (Anderson, Lowell & Prieve 1982; Israelachvili 2011), denoted by L , is the typical length scale over which ϕ decays away from the surface. For ions, the diffuse layer is referred to as the electric double layer, ϕ is the electrostatic potential and $L = \lambda_D$, the Debye layer thickness. In a $z : z$ electrolyte solution (z is the ion valence) with a solute concentration c and dielectric constant ϵ , the Debye layer thickness is (Prieve *et al.* 1984)

$$\lambda_D = \sqrt{\frac{\epsilon k_B T}{2z^2 e^2 c}}, \quad (2.1)$$

where e is the electric charge, k_B is the Boltzmann constant and T is the absolute temperature.

When the diffuse layer thickness L is much smaller than the radius of a spherical particle a , a slip velocity, at the outer boundary of the diffuse layer, can be assumed on the particle due to diffusiophoresis. For non-electrolytes, this slip velocity \mathbf{v} at position \mathbf{x} is solely determined by chemiphoresis, or pressure gradients established by osmotic effects, which is (Derjaguin *et al.* 1947; Anderson 1989; Michelin & Lauga 2014; Mozaffari *et al.* 2016)

$$\mathbf{v}_s(\mathbf{x}) = -\frac{k_B T L^2}{\mu} \int_0^\infty y \left[\exp\left(-\frac{\phi(y)}{k_B T}\right) - 1 \right] dy \nabla_s c, \quad (2.2)$$

where μ is the fluid viscosity, ∇_s is the gradient operator along the surface and c is the solute concentration field at the outer boundary of the diffuse layer. Here, the dimensionless coordinate $y = (r_n - a)/L$ is normal to the surface, where r_n is the normal coordinate. The potential distribution $\phi(y)$ is determined by interactions of the solute with the surface. For electrolytes, the slip velocity is (Prieve *et al.* 1984)

$$\mathbf{v}_s(\mathbf{x}) = -\frac{k_B T L^2}{\mu} \left[-2\beta\zeta + \frac{4k_B T}{ze} \ln(1 - \gamma^2) \right] \nabla_s c, \quad (2.3)$$

with

$$\beta = \frac{D_+ - D_-}{D_+ + D_-} \quad \text{and} \quad \gamma = \tanh\left(\frac{ze\zeta}{k_B T}\right), \quad (2.4a,b)$$

where D_+ (D_-) is the diffusivity of the cations (anions) and ζ is the zeta potential of the particle. We note that the second term in (2.3) is just an explicit form of (2.2), when ϕ is the electrostatic potential, while the first term in (2.3) is due to electrophoresis (Prieve *et al.* 1984); the difference in diffusivities of the cations and anions ($\beta \neq 0$) generates an electric field when there is a concentration gradient, and the electric field moves the particle. Therefore, diffusiophoresis in an electrolyte solution consists of both chemiphoretic and electrophoretic contributions (Prieve *et al.* 1984; Anderson 1989).

Many papers (Golestanian *et al.* 2007; Michelin & Lauga 2014, 2015; Schnitzer & Yariv 2015; Mozaffari *et al.* 2016; Yariv 2016) in the study of diffusiophoresis use the slip velocity

$$\mathbf{v}_s(\mathbf{x}) = b \nabla_s c, \quad (2.5)$$

by assuming that the diffuse layer thickness L and so

$$b = -\frac{k_B T L^2}{\mu} \int_0^\infty y \left[\exp\left(-\frac{\phi(y)}{k_B T}\right) - 1 \right] dy \quad (2.6)$$

are constants. The form of the slip velocity (2.5) together with (2.6) was first derived by Derjaguin *et al.* (1947) for flat-plane geometry and was shown to be true at leading order in L/a for a spherical particle by Anderson *et al.* (1982), where L is defined as the range of the solute–particle interaction. We note that the typical L for many intermolecular potentials ϕ also depends on the local solute concentration c . For example, L for electrostatic interactions is just the Debye length, i.e.

$$L = \lambda_D \propto c^{-1/2}, \quad (2.7)$$

as given in (2.1). As a result, the prefactor b in (2.5) is not a constant but a function of c . An appropriate form of the slip velocity for diffusiophoresis in electrolyte solutions, by taking the variation of L along the particle surface into account, is (Prieve *et al.* 1984; Anderson 1989)

$$\mathbf{v}_s(\mathbf{x}) = \chi \nabla_s \ln c, \quad (2.8)$$

in which

$$\chi = -\frac{\epsilon(k_B T)^2}{2\mu(z_e)^2} \left[-2\beta\zeta + \frac{4k_B T}{z_e} \ln(1 - \gamma^2) \right] \quad (2.9)$$

is constant. Here, χ is referred to as the particle mobility.

It has been found experimentally that the autophoretic speeds of Pt/insulator (Ebbens *et al.* 2014) and Pt/Au (Paxton *et al.* 2006; Moran & Posner 2014) Janus particles can be significantly decreased by adding a small amount of salt, which can be mainly explained by the combination of two mechanisms. The first is that the addition of salt changes the surface chemical reactions (Ebbens *et al.* 2014) and the second is that the autophoretic speed is proportional to the inverse of the conductivity S of the bulk solution (Paxton *et al.* 2006; Moran & Posner 2014). Since $S^{-1} \propto \lambda_D^2$ with λ_D the Debye length, the autophoretic speed should be proportional to λ_D^2 , which agrees with the slip velocity expressions (2.3), (2.8) and (2.9).

Within the diffuse layer, there are mainly five types of interactions driving the flow: solute/solute, solute/solvent, solute/colloid, solvent/solvent and solvent/colloid interactions. In electrolyte diffusiophoresis, only the electrostatic interactions associated with solute/solute and solute/colloid interactions are considered (Prieve *et al.* 1984), which results in the diffuse layer thickness $L \sim c^{-1/2}$. However, in classical non-electrolyte diffusiophoresis, only solute/colloid and solvent/colloid interactions are considered and the solute/solute interaction is neglected by assuming dilute solutions, which makes L independent of c (Sharifi-Mood *et al.* 2013). In the general case, L will depend on the solute concentration, solvent and colloid properties and therefore also on the relative strengths of the different interactions, although we note that the dependence of L on c may be a higher-order effect for non-electrolyte diffusiophoresis.

We note that both (2.2) and (2.3) are derived by assuming local equilibrium within the diffuse layer, i.e. there is no desorption or adsorption flux. However, it has been shown that the effect of a non-zero diffusive flux within the diffuse layer on the slip velocity is only $O(L/a)$ for $L/a \ll 1$ for both ionic autophoresis (Rubinstein & Zaltzman 2001; Zaltzman & Rubinstein 2007) and non-ionic autophoresis (Sabass & Seifert 2012; Sharifi-Mood *et al.* 2013; Michelin & Lauga 2014; Shklyaev *et al.* 2014). Therefore, (2.2) and (2.3) are still valid to leading order when $L/a \ll 1$.

We demonstrate this idea, i.e. that the solute flux does not change the leading-order expression of the slip velocity, in appendix A.

3. Reciprocal theorem

In this section, we assume that the slip velocity distribution (2.8) is known on the surfaces of the particles, which here are assumed to be two spheres of equal radius. Then, we will show that accounting for hydrodynamic interactions, the velocities of the two spheres in a Stokes flow can be computed through the reciprocal theorem.

Consider two spherical particles O_1 and O_2 , each with radius a , which are steadily adsorbing ions from or desorbing ions into an unbounded electrolyte solution, as shown in figure 1. The particle surfaces are denoted by S_1 and S_2 , respectively. A spherical coordinate system is fixed onto the centre of O_1 . We want to study the interaction of the two particles due to the asymmetric solute concentration field that is established.

The translation velocities of the two particles are denoted as $\mathbf{v}_{p,1}$ and $\mathbf{v}_{p,2}$, respectively. Then, the fluid velocity on the particle surfaces can be written as

$$\mathbf{v}_1(\mathbf{x}) = \mathbf{v}_{p,1} + \mathbf{v}_{s,1}(\mathbf{x}), \quad (3.1a)$$

$$\text{and } \mathbf{v}_2(\mathbf{x}) = \mathbf{v}_{p,2} + \mathbf{v}_{s,2}(\mathbf{x}), \quad (3.1b)$$

respectively, where $\mathbf{v}_{s,i}$ ($i = 1, 2$) is the slip velocity on particle i . As discussed in the introduction, the slip velocities for electrolyte solutions have the form (2.8), i.e.

$$\mathbf{v}_{s,i} = \chi_i \nabla_s \ln c, \quad (3.2)$$

where χ_i is constant when the surface charge (or the zeta potential) is uniform on the particles, and c is the concentration field, which can vary along the surface. The final goal is to calculate $\mathbf{v}_{p,i}$ for a concentration field determined by the two particles.

The typical diffusiophoretic speed of colloids ($a \approx 1 \mu\text{m}$) in an aqueous solution is of the order of $1 \mu\text{m s}^{-1}$ (Palacci *et al.* 2010; Shin *et al.* 2016). Therefore, the particle-scale Reynolds number $Re = O(10^{-6})$ and the flow field is governed by the Stokes equations, assuming incompressible flow, i.e.

$$\nabla \cdot \boldsymbol{\sigma} = \mathbf{0}, \quad (3.3a)$$

$$\nabla \cdot \mathbf{v} = 0, \quad (3.3b)$$

where $\boldsymbol{\sigma}$ is the stress tensor and \mathbf{v} is the fluid velocity. The Lorentz reciprocal theorem is

$$\int_S \mathbf{n} \cdot \boldsymbol{\sigma}' \cdot \mathbf{v} \, dS = \int_S \mathbf{n} \cdot \boldsymbol{\sigma} \cdot \mathbf{v}' \, dS, \quad (3.4)$$

where \mathbf{v}' and $\boldsymbol{\sigma}'$, respectively, are the velocity and stress fields for a model problem with different boundary conditions on the boundary surfaces S , including the surfaces S_i of particle $i = 1, 2$. The domain of integration for (3.4) is $S = S_1 + S_2 + S_\infty$, where S_∞ is a surface at infinity enclosing both particles and the normal vector \mathbf{n} points away from the particle into the fluid, as shown in figure 1(a).

In the sections below, we choose our model problem as two uncharged particles translating either towards each other or at the same velocity. In either case, \mathbf{v}' is constant and can be taken out of the integral in (3.4), and the integral $\int \mathbf{n} \cdot \boldsymbol{\sigma} \, dS$

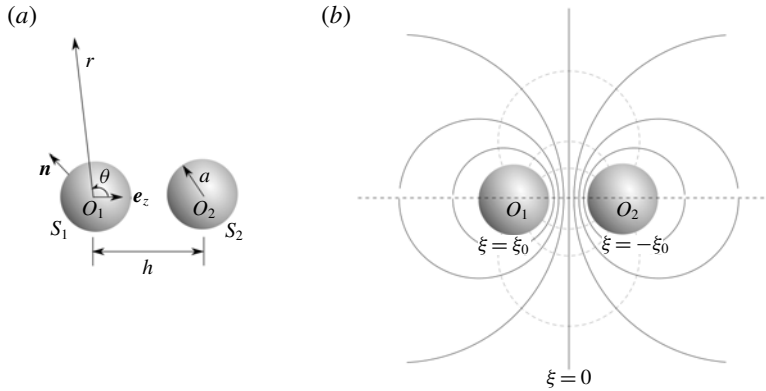


FIGURE 1. Model set-up. (a) Two spheres O_1 and O_2 each with radius a are suspended in an infinite fluid field with an initial separation distance between the centres h . Their surfaces are labelled by S_1 and S_2 , respectively, with the unit normal denoted by \mathbf{n} . A spherical coordinate system is fixed at O_1 and \mathbf{e}_z is a unit vector directed from O_1 to O_2 . (b) The bi-spherical coordinate system represented by (6.1). The solid (dashed) lines indicate the surfaces of constant ξ (η) and $\xi = \pm\xi_0$ represents the surfaces S_1 and S_2 , respectively.

is the hydrodynamic force on the particles and their electric double layers, which is zero (Prieve *et al.* 1984). Therefore, we have (Stone & Samuel 1996)

$$\int_S \mathbf{n} \cdot \boldsymbol{\sigma}' \cdot \mathbf{v} \, dS = \int_S \mathbf{n} \cdot \boldsymbol{\sigma} \cdot \mathbf{v}' \, dS = \mathbf{v}' \cdot \int_S \mathbf{n} \cdot \boldsymbol{\sigma} \, dS = 0. \tag{3.5}$$

Substituting (3.2) and (3.1) into (3.5), we have

$$\begin{aligned} 0 = & \mathbf{v}_{p,1} \cdot \int_{S_1} \mathbf{n} \cdot \boldsymbol{\sigma}' \, dS + \mathbf{v}_{p,2} \cdot \int_{S_2} \mathbf{n} \cdot \boldsymbol{\sigma}' \, dS + \chi_1 \int_{S_1} \mathbf{n} \cdot \boldsymbol{\sigma}' \cdot \nabla_s \ln c \, dS \\ & + \chi_2 \int_{S_2} \mathbf{n} \cdot \boldsymbol{\sigma}' \cdot \nabla_s \ln c \, dS. \end{aligned} \tag{3.6}$$

In deriving (3.6), we use the fact that the surface integral at infinity is zero because the integrand decays sufficiently fast to a fluid at rest. Now we consider two special cases: (i) $\chi_1 = \chi_2$ and (ii) $\chi_1 = -\chi_2$. Then, for arbitrary mobilities χ_1 and χ_2 , the velocity of each particle $\mathbf{v}_{p,i}$ is a linear combination of these two special cases.

3.1. Case (i): $\chi_1 = \chi_2$

We choose a low-Reynolds-number model problem (i) as two uncharged particles translating towards each other at velocity \mathbf{v}'_a . This problem is identical to a single sphere translating towards a symmetry plane and has a well-known solution (Brenner 1961). Also, due to symmetry of the concentration field for the two particles adsorbing/desorbing ionic solute, we have $\mathbf{v}_{p,1} = -\mathbf{v}_{p,2}$ and

$$\int_{S_1} \mathbf{n} \cdot \boldsymbol{\sigma}'_a \, dS = - \int_{S_2} \mathbf{n} \cdot \boldsymbol{\sigma}'_a \, dS, \tag{3.7a}$$

$$\int_{S_1} \mathbf{n} \cdot \boldsymbol{\sigma}'_a \cdot \nabla_s \ln c \, dS = \int_{S_2} \mathbf{n} \cdot \boldsymbol{\sigma}'_a \cdot \nabla_s \ln c \, dS, \tag{3.7b}$$

where σ'_a is the stress field for model problem (i). By defining the hydrodynamic force $f'_{H,a} = \int_{S_1} \mathbf{n} \cdot \sigma'_a dS$, with (3.7), equation (3.6) becomes

$$\mathbf{v}_{p,1} \cdot \mathbf{f}'_{H,a} = -\chi_1 \int_{S_1} \mathbf{n} \cdot \sigma'_a \cdot \nabla_s \ln c dS. \tag{3.8}$$

Because of the symmetry of the two-sphere configuration, $\mathbf{v}_{p,1}$ is parallel to $\mathbf{f}'_{H,a}$, and we have

$$\mathbf{v}_{p,1} = -\mathbf{v}_{p,2} = \chi_1 \mathbf{v}_+ = -\frac{\chi_1}{|\mathbf{f}'_{H,a}|^2} \mathbf{f}'_{H,a} \int_{S_1} \mathbf{n} \cdot \sigma'_a \cdot \nabla_s \ln c dS, \tag{3.9}$$

which serves to define \mathbf{v}_+ .

3.2. Case (ii): $\chi_1 = -\chi_2$

We choose a model problem (ii) as two uncharged particles translating at the same velocity \mathbf{v}'_b in a Stokes flow, for which the flow field is given by Stimson & Jeffery (1926). Similarly, due to symmetry, we have $\mathbf{v}_{p,1} = \mathbf{v}_{p,2}$ and

$$\int_{S_1} \mathbf{n} \cdot \sigma'_b dS = \int_{S_2} \mathbf{n} \cdot \sigma'_b dS, \tag{3.10a}$$

$$\int_{S_1} \mathbf{n} \cdot \sigma'_b \cdot \nabla_s \ln c dS = - \int_{S_2} \mathbf{n} \cdot \sigma'_b \cdot \nabla_s \ln c dS, \tag{3.10b}$$

where σ'_b is the stress field for model problem (ii). Similar to the steps in § 3.1, by defining $\mathbf{f}'_{H,b} = \int_{S_1} \mathbf{n} \cdot \sigma'_b dS$, with (3.10), equation (3.6) then becomes

$$\mathbf{v}_{p,1} \cdot \mathbf{f}'_{H,b} = -\chi_1 \int_{S_1} \mathbf{n} \cdot \sigma'_b \cdot \nabla_s \ln c dS, \tag{3.11}$$

i.e.

$$\mathbf{v}_{p,1} = \mathbf{v}_{p,2} = \chi_1 \mathbf{v}_- = -\frac{\chi_1}{|\mathbf{f}'_{H,b}|^2} \mathbf{f}'_{H,b} \int_{S_1} \mathbf{n} \cdot \sigma'_b \cdot \nabla_s \ln c dS, \tag{3.12}$$

which defines \mathbf{v}_- .

3.3. Arbitrary χ_1 and χ_2

For arbitrary constant values of χ_1 and χ_2 , we use the decomposition

$$\chi_1 = \frac{\chi_1 + \chi_2}{2} + \frac{\chi_1 - \chi_2}{2}, \tag{3.13a}$$

$$\chi_2 = \frac{\chi_1 + \chi_2}{2} - \frac{\chi_1 - \chi_2}{2}, \tag{3.13b}$$

together with (3.9) and (3.12). Thus, we have

$$\mathbf{v}_{p,1} = \frac{\chi_1 + \chi_2}{2} \mathbf{v}_+ + \frac{\chi_1 - \chi_2}{2} \mathbf{v}_-, \tag{3.14a}$$

$$\mathbf{v}_{p,2} = -\frac{\chi_1 + \chi_2}{2} \mathbf{v}_+ + \frac{\chi_1 - \chi_2}{2} \mathbf{v}_-, \tag{3.14b}$$

where \mathbf{v}_+ and \mathbf{v}_- are determined by $\nabla_s \ln c$ and the geometry, i.e. σ'_a and σ'_b . Now, for a spherical particle in an axisymmetric configuration it suffices to determine the concentration field $c(r, \theta, t)$ after which \mathbf{v}_- and \mathbf{v}_+ follow, respectively, from (3.9) and (3.12). Note that the linear superposition in (3.14) is only valid when the governing equations and corresponding boundary conditions for both the velocity and concentration fields are linear. The Stokes equations are linear for the velocity field, and conditions for the linearity of the equations governing the concentration field will be discussed with (4.1) and (4.2) in the next section.

4. Concentration field: governing equations and boundary conditions

The typical diffusiophoretic velocity is $u \approx 1 \mu\text{m s}^{-1}$ (Palacci *et al.* 2010; Shin *et al.* 2016) and the typical diffusivity for ions is $D \approx 10^{-9} \text{m}^2 \text{s}^{-1}$ (Bird, Stewart & Lightfoot 1960). For particles with radius $a \approx 1 \mu\text{m}$, the Péclet number $Pe = au/D \approx 10^{-3} \ll 1$. Thus, we can neglect the advection of ions when considering the transport of solute. Assuming that c adjusts quasi-statically to changes in geometry, the governing equation and boundary conditions for the concentration field are

$$\nabla^2 c = 0. \quad (4.1)$$

Since the emphasis of this paper is on the effects of a slip velocity, we assume the sorption kinetics satisfies the zero-order model, i.e. the sorption flux j is constant. We note that it is straightforward to generalize the uniform-flux model by considering any axisymmetric flux profile over the particle surface, which can be achieved by decomposing the flux distribution into a series of Legendre polynomials (Tătulea-Codrean & Lauga 2018). It can be shown that at the outer boundary of the diffuse layer, the diffusive flux satisfies (Yariv 2011; Michelin & Lauga 2014)

$$-D \frac{\partial c}{\partial r} = j \quad \text{at } S_1 \text{ and } S_2, \quad (4.2)$$

where the diffusion coefficient in (4.2) is

$$D = \frac{2D_+D_-}{D_+ + D_-}. \quad (4.3)$$

Recall that D_+ and D_- are the diffusivity of cations and anions, respectively. Equation (4.2) serves as the boundary condition for the concentration field at the particle surface in the limit $L \ll a$. We note that j can be either positive or negative, corresponding to desorption or adsorption of solute, respectively. The boundary condition (4.2) can also be used for surface chemical reactions (e.g. catalysts) satisfying Michaelis–Menten kinetics when the reactant concentration is large (Michaelis & Menten 1913; Johnson & Goody 2011), or any kinetics satisfying a zero-order model (Dash *et al.* 2010). It is convenient to define an unperturbed concentration of ions c_∞ and an excess concentration $c_e = c - c_\infty$, which is positive for desorption and negative for adsorption of solutes. Then (4.2) becomes

$$D \frac{\partial c_e}{\partial r} = -j. \quad (4.4)$$

Based on (4.4), we define $\Delta c = ja/D$ as the typical scale for c_e . In electrolyte solutions, using (2.6), $\mathbf{v}_s \propto \nabla_s c$, instead of (2.8), $\mathbf{v}_s \propto \nabla_s \ln c$, leads to errors of order $\Delta c/c_\infty$. As a result, we will show the asymmetric effects of adsorption and desorption

and the saturation of the autophoretic velocity for large adsorption fluxes (j). In the following analysis, we first calculate the autophoresis of two adsorbing/desorbing particles asymptotically when they are far apart ($h \gg a$), then for arbitrary distances $h > 2a$ in bi-spherical coordinates.

It is straightforward to non-dimensionalize the excess concentration field by ja/D . The typical length scale is a and, from (2.8), the typical velocity is χ_1/a . Then we can non-dimensionalize forces by $\mu\chi_1$ and stresses by $\mu\chi_1/a^2$. We introduce dimensionless variables

$$\left. \begin{aligned} C &= \frac{c}{c_\infty}, & C_e &= \frac{Dc_e}{ja}, & R &= \frac{r}{a}, & H &= \frac{h}{a}, \\ J &= \frac{\Delta c}{c_\infty} = \frac{ja}{c_\infty D}, & U &= \frac{au}{\chi_1}, & F &= \frac{f}{\mu\chi_1}, & \Sigma &= \frac{a^2\sigma}{\mu\chi_1}. \end{aligned} \right\} \tag{4.5}$$

We note that the background concentration c_∞ and the excess concentration c_e are scaled differently in (4.5), by a factor of J ; therefore, the dimensionless concentration field can be written as

$$C = 1 + JC_e. \tag{4.6}$$

The corresponding non-dimensional equation for the concentration distribution is

$$\nabla^2 C_e = 0 \tag{4.7}$$

with boundary conditions

$$\frac{\partial C_e}{\partial n} = -1 \quad \text{at } S_1 \text{ and } S_2, \tag{4.8a}$$

$$C_e = 0 \quad \text{as } R \rightarrow \infty. \tag{4.8b}$$

5. Asymptotic analysis: $H \gg 1$

In this section, we calculate the autophoretic particle velocity for the asymptotic case of large separation distance, i.e. when $H = h/a \gg 1$, and use the method of reflections to solve for the concentration field. The presence of the second particle breaks the symmetry and induces translation of the particles. We use a spherical coordinate system centred on sphere O_1 , as shown in figure 1(a). In the absence of sphere O_2 , the excess concentration field, which satisfies (4.7) to (4.8b), is

$$C_{e1}^{(0)}(\mathbf{R}) = \frac{1}{R}, \tag{5.1}$$

where \mathbf{R} is the dimensionless position vector and the superscript ‘ (n) ’ indicates the solution under the n th reflection. Similarly, the excess concentration induced by sphere O_2 in the absence of O_1 is

$$C_{e2}^{(0)} = \frac{1}{|\mathbf{R} - H\mathbf{e}_z|} = \frac{1}{H} + \frac{\mathbf{e}_z \cdot \mathbf{R}}{H^2} + O(H^{-3}), \tag{5.2}$$

where \mathbf{e}_z is the unit vector pointing from O_1 to O_2 , as shown in figure 1(a), and we assume $H \gg 1$. The reflection of the field C_{e2} due to the presence of O_1 , denoted by $C_{e2}^{(1)}$, is

$$C_{e2}^{(1)} = \frac{\mathbf{e}_z \cdot \mathbf{R}}{2H^2R^3} + O(H^{-3}). \tag{5.3}$$

Thus, the dimensionless concentration field in the vicinity of the sphere O_1 (i.e. $R = O(1)$) is

$$C(\mathbf{R}) = 1 + JC_e = 1 + J \left(\frac{1}{R} + \frac{1}{H} \right) + \frac{J}{H^2} \left(1 + \frac{1}{2R^3} \right) \mathbf{e}_z \cdot \mathbf{R} + O(H^{-3}). \quad (5.4)$$

Note that the scalings of C_e and C are different by a factor of J in (4.5). By symmetry, the surface integral of the slip velocity on sphere O_1 is

$$\int_{S_1} \nabla_s \ln C \, dS = \frac{4\pi J}{(1+J)H^2} \mathbf{e}_z + O(H^{-3}). \quad (5.5)$$

At leading order for $H \gg 1$, the stress distributions on the particle surfaces of both model problems (i) and (ii) are the same as that of a single sphere translating through an unbounded fluid under a (dimensionless) hydrodynamic force \mathbf{F}' . A well-known result for this problem is (Leal 2007)

$$4\pi \mathbf{n} \cdot \boldsymbol{\Sigma}' = \mathbf{F}', \quad (5.6)$$

where $\boldsymbol{\Sigma}'$ is the constant surface stress vector on the sphere surface. Therefore, based on the reciprocal theorem (3.8) and (5.5), the velocity of particle 1 is

$$\mathbf{U}_{p,1} = -\frac{J}{(1+J)H^2} \mathbf{e}_z, \quad (5.7)$$

where we only keep the leading-order $O(H^{-2})$ terms. We notice that a similar asymptotic analysis for non-electrolyte autophoresis was given by Yariv (2016), who adopted the formula of slip velocity (2.5) to obtain

$$\mathbf{U}_{p,1}^{ne} = -\frac{J}{H^2} \mathbf{e}_z. \quad (5.8)$$

This result can be obtained from (5.7) in the limit $|J| \ll 1$. A comparison of these two velocities is plotted in figure 2.

The non-electrolyte result (5.8) will increase without bound when $J = ja/Dc_\infty \rightarrow \infty$, because (2.5) leads to the largest deviation in this limit, as discussed at the end of §4. On the other hand, the autophoretic velocities produced by desorption fluxes ($J > 0$) in electrolyte solutions are bounded by H^{-2} , as shown in figure 2. For adsorption fluxes $J < 0$, figure 2 shows that the autophoretic velocity will grow superlinearly and diverges as $J \rightarrow -1$, because the concentration field at the particle surfaces $C \rightarrow 0$ as $J \rightarrow -1$, which results in a large slip velocity $\nabla \ln C \rightarrow \infty$. As shown in figure 2, our theoretical results from numerical integration of (6.10) in §6 are in good agreement with the asymptotic results except for near $J \rightarrow -1$ where the autophoretic velocity diverges and higher-order corrections in (5.5) are no longer negligible. Since our analysis is based on the assumption of a thin Debye layer, our results are valid for $\lambda_D/a \ll 1$. When the two particles are far apart ($H \gg 1$), with (2.1), (4.5) and (5.4), the thin-Debye-layer criterion with sorption fluxes becomes

$$\left(\frac{\lambda_{D\infty}}{a} \right)^2 \ll 1 + J, \quad (5.9)$$

where

$$\lambda_{D\infty} = \sqrt{\frac{\epsilon k_B T}{2z^2 e^2 c_\infty}} \quad (5.10)$$

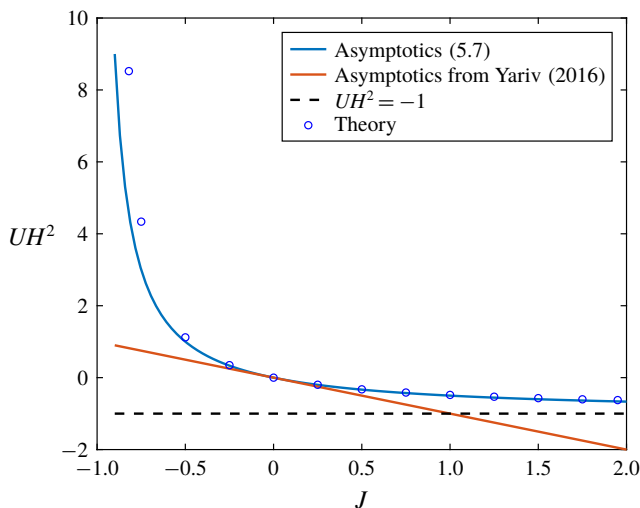


FIGURE 2. (Colour online) Asymptotic results based on (5.7) and (5.8) for the autophoretic velocity, plotted as UH^2 , as functions of J . The dashed line $UH^2 = -1$ is the lower limit of (5.7) and the open circles are theoretical results calculated by numerical integration of (6.10). Here $H = 10$ for all the curves plotted.

is the unperturbed Debye length. Therefore, $J > -1$ must be satisfied for adsorption fluxes because the solute concentration cannot be negative near the particles. For a typical system with $\lambda_{D\infty} = 10$ nm and $a = 1$ μm , the thin-Debye-layer criterion (5.10) requires that $1 + J \gg 10^{-8}$, which means that the thin-Debye-layer assumption can still hold as $J \rightarrow -1$ when the particles are far apart. The analysis in appendix A gives an upper limit of J in (A 6). For the same system ($\lambda_{D\infty} = 10$ nm and $a = 1$ μm), (A 6) requires that $J \ll 10^4$. Typical values of desorption flux j measured in experiments are around $7 \times 10^{-6} - 4 \times 10^{-2}$ mol (m² s)⁻¹ (Paxton *et al.* 2005; Howse *et al.* 2007; Sen *et al.* 2009; Wang *et al.* 2013; Brown & Poon 2014), for particles with radius $a = 1$ μm in an electrolyte solution with background concentration $c_\infty = 0.1$ mM and diffusion coefficient $D = 1 \times 10^{-9}$ m² s⁻¹. The concomitant range of J is between 7×10^{-2} and 4×10^2 , where the theory for non-ionic solvents severely over- or under-predicts the phoretic motion (e.g. see figure 2), whereas our theory should be applicable to many experiments with large J .

We note that when the flux J is large, steric effects may be significant due to a high solute concentration (Kilic *et al.* 2007). For non-desorbing particles, the ionic steric effects can be characterized by the packing parameter $\nu = 2d_{ion}^3 c_\infty$ (Kilic *et al.* 2007; Figliuzzi *et al.* 2014), with d_{ion} the ionic diameter and c_∞ the bulk solution concentration far away from the particle. For particles with a desorption flux j , we replace c_∞ with $c_\infty + ja/D$ to estimate the effects of the flux on the background concentration, so the packing parameter for desorbing particles can be written as $\nu' = 2d_{ion}^3 c_\infty (1 + J)$. Steric effects can be neglected when $\nu' \ll 1$. The typical value of d_{ion} for potassium, sodium and chloride ions is ≈ 1 Å (Mancinelli *et al.* 2007). For a typical background concentration $c_\infty = 0.1$ M, we have $d_{ion}^3 c_\infty \approx 6 \times 10^{-5}$. Therefore, steric effects can be neglected when $J \ll 10^4$. We remark that this limit is greater than those typically realized in experiments, as discussed above.

Moreover, the expression (5.8) predicts that the effects of adsorption and desorption fluxes J are symmetric to the autophoresis, with only a difference of sign. However,

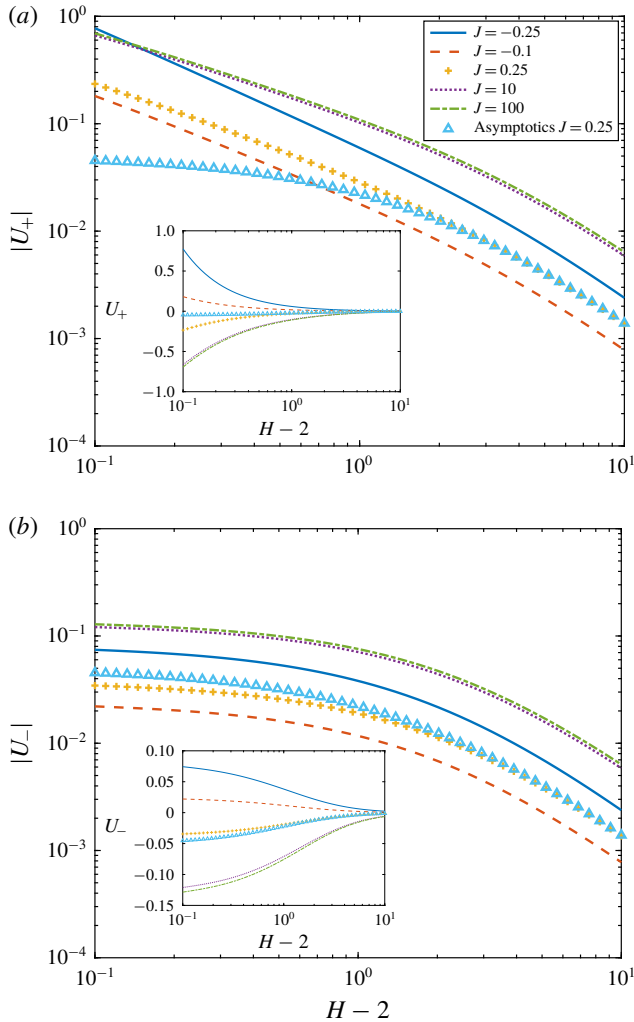


FIGURE 3. (Colour online) Dependence of (a) $|U_+|$ and (b) $|U_-|$ on $H - 2$ for different sorption flux J . Insets show values of (a) U_+ and (b) U_- . The asymptotic result for $J = 0.25$ is determined according to (5.7) and the other curves are theoretical results obtained by numerical calculation of (6.10).

this is not true for an electrolyte solution when $\mathbf{v}_s \propto \nabla_s \ln c$ and the resultant autophoretic velocity (5.7) shows that an adsorption flux $J < 0$ is more effective in creating stronger autophoresis because it decreases the mean concentration around the particles. We note that the results of Yariv (2016) are recovered as a limit of our theory for $|J| \ll 1$. The asymmetric contributions of desorption and adsorption fluxes will also be illustrated in figure 3 in the next section, where we provide an analysis for an arbitrary separation distance H .

6. General case: an arbitrary distance H

Laplace's equation (4.7) in an unbounded fluid with two identical spherical boundaries can be solved in a bi-spherical coordinate system (Jeffery 1912) and

is well known. By defining $\xi_0 = \text{arccosh}(H/2)$, which establishes the separation distance, the transformation from the cylindrical coordinate system (R, Z, ϕ) to the bi-spherical coordinate system (ξ, η, ϕ) is given by

$$R = \frac{\sinh \xi_0 \sin \eta}{\cosh \xi - \cos \eta}, \quad Z = \frac{\sinh \xi_0 \sinh \xi}{\cosh \xi - \cos \eta}. \quad (6.1a,b)$$

The particle surfaces S_1 and S_2 can be described by $\xi = \pm \xi_0$ in this coordinate system, as shown in figure 1(b). By further changing variable $\tau = \cos \eta$, the solution to the Laplace equation (4.7) in bi-spherical coordinates is (Jeffery 1912; Michelin & Lauga 2015)

$$C_e(\xi, \tau) = (\cosh \xi - \tau)^{1/2} \sum_{n=0}^{\infty} f_n(\xi) P_n(\tau), \quad (6.2)$$

where P_n is the Legendre polynomial of degree n and

$$f_n(\xi) = 2\gamma_n e^{-(n+1/2)\xi_0} \cosh(n + \frac{1}{2})\xi, \quad (6.3)$$

in which γ_n are constant. The coefficients γ_n can be further determined by the boundary conditions (4.8a)

$$\frac{(\cosh \xi - \tau)}{\sinh \xi_0} \frac{\partial C_e}{\partial \xi} = 1 \quad \text{at } \xi = \xi_0. \quad (6.4)$$

Due to symmetry, using the flux boundary condition on S_1 is sufficient to determine the concentration field. Equation (6.4) can be written explicitly as

$$\frac{\sinh \xi_0}{2 \sinh \xi_0} C_e + \frac{(\cosh \xi_0 - \tau)^{3/2}}{\sinh \xi_0} \sum_{n=0}^{\infty} \frac{df_n}{d\xi}(\xi_0) P_n(\tau) = 1, \quad (6.5)$$

which after substituting for C_e with (6.2) yields

$$\sum_{n=0}^{\infty} \left[\frac{\sinh \xi_0}{2 \sinh \xi_0} f_n(\xi_0) + \frac{\cosh \xi_0 - \tau}{\sinh \xi_0} \frac{df_n}{d\xi}(\xi_0) \right] P_n(\tau) = (\cosh \xi_0 - \tau)^{-1/2}. \quad (6.6)$$

Using the properties of Legendre polynomials listed in appendix B, we have

$$\begin{aligned} & \frac{1}{2} f_n(\xi_0) + \frac{df_n}{d\xi}(\xi_0) \coth \xi_0 - \frac{1}{\sinh \xi_0} \left[\frac{n+1}{2n+3} \frac{df_{n+1}}{d\xi}(\xi_0) + \frac{n}{2n-1} \frac{df_{n-1}}{d\xi}(\xi_0) \right] \\ & = \sqrt{2} e^{-(n+1/2)\xi_0}. \end{aligned} \quad (6.7)$$

Substituting (6.3) into (6.7), we obtain a recursion relation for the coefficients γ_n :

$$\begin{aligned} \gamma_{n+1} = & \frac{e^{\xi_0}}{(n+1) \sinh(n + \frac{3}{2})\xi_0} \left\{ \left[\sinh \xi_0 \cosh \left(n + \frac{1}{2} \right) \xi_0 \right. \right. \\ & + (2n+1) \cosh \xi_0 \sinh \left(n + \frac{1}{2} \right) \xi_0 \left. \right] \gamma_n \\ & \left. - n e^{\xi_0} \gamma_{n-1} \sinh \left(n - \frac{1}{2} \right) \xi_0 - \sqrt{2} \sinh \xi_0 \right\}. \end{aligned} \quad (6.8)$$

We solve the linear system (6.8) numerically for the coefficients γ_n .

For both model problems (i) and (ii), the normal stress can be written as (Rallabandi, Hilgenfeldt & Stone 2017)

$$\mathbf{n} \cdot \boldsymbol{\Sigma} = -P'\mathbf{n} + \Omega's, \quad (6.9)$$

where s is the unit tangent vector on the sphere, P' is the pressure and Ω' is the vorticity. Based on (3.9) and (3.12), by defining the mobility ratio $\alpha = \chi_2/\chi_1$, we find that the velocities of particle 1 for the cases $\alpha = \pm 1$ are

$$U_+ = -2\pi F_{H,a}^{-1} \int_{-1}^1 R(\xi_0, \tau) \Omega'_a(\xi_0, \tau) \frac{J}{1 + J C_e(\xi_0, \tau)} \frac{\partial C_e(\xi_0, \tau)}{\partial \tau} d\tau, \quad (6.10a)$$

$$U_- = -2\pi F_{H,b}^{-1} \int_{-1}^1 R(\xi_0, \tau) \Omega'_b(\xi_0, \tau) \frac{J}{1 + J C_e(\xi_0, \tau)} \frac{\partial C_e(\xi_0, \tau)}{\partial \tau} d\tau, \quad (6.10b)$$

respectively, where F_H is the hydrodynamic force on the sphere and the subscript a or b represents the corresponding model problem. The expressions of $F_{H,a}$, $F_{H,b}$, $\Omega'_a(\xi, \tau)$ and $\Omega'_b(\xi, \tau)$ are listed in appendix C. Then, for arbitrary α , the velocities of particle 1 and 2 are

$$U_{p,1} = \frac{(1 + \alpha)}{2} U_+ + \frac{(1 - \alpha)}{2} U_-, \quad (6.11a)$$

$$U_{p,2} = -\frac{(1 + \alpha)}{2} U_+ + \frac{(1 - \alpha)}{2} U_-, \quad (6.11b)$$

respectively (see (3.14) for the dimensional form).

We compute the integrals in (6.10) numerically using (6.2), (6.3) and coefficients γ_n obtained from (6.8). The dependence of solute fluxes J on the autophoretic speeds is shown and compared with the asymptotic solution (5.7) in figure 3. We find that the magnitude of the autophoretic velocity induced by adsorption fluxes, i.e. $J < 0$, is stronger than that induced by desorption fluxes, since adsorption fluxes result in a smaller concentration field and increase $\nabla \ln C$. In figure 3, as J increases, the autophoretic speeds converge to a finite value as opposed to diverging; since the slip velocity is proportional to $\nabla_s \ln C$, increasing J will increase both ∇C and C and consequently the slip velocity will converge to a finite value as $J \rightarrow \infty$. The boundedness of autophoretic speeds with respect to J is consistent with the asymptotic result (5.7). For the large fluxes in self-propelling systems with ion adsorption or desorption, the phoretic velocity does not depend linearly on the flux. There is a saturation for desorption and a superlinear increase of velocity with adsorption flux.

7. Concluding remarks

In this paper, we have shown that the typical thickness L over which the intermolecular potential decays away from the particle surface is generally not constant but depends on the local concentration field along the particle surface. We review different expressions of diffusiophoretic slip velocities in electrolyte and non-electrolyte solutions and find that when the sorption fluxes are large enough to modify the solute concentration, i.e. $J = ja/c_\infty D$ is $O(1)$ or greater, and consequently the interaction layer on particle surfaces, the assumption of a slip velocity $\mathbf{v}_s \propto \nabla_s c$ will lead to significant errors. For autophoresis of two particles in an electrolyte solution with $\mathbf{v}_s \propto \nabla_s \ln c$, we show, both asymptotically and analytically, that

the phoretic velocities due to adsorption and desorption are asymmetric, in the sense that not only are the directions opposite, but also the trends for increasing adsorption and desorption fluxes are different. For particles desorbing ionic solute, the phoretic velocity saturates with increasing desorption fluxes. On the other hand, the magnitude of the autophoretic velocity for two identical particles that adsorb solutes grows superlinearly with adsorption flux. These conclusions are in contrast with the symmetric results of autophoresis in a non-electrolyte solution reported in Michelin & Lauga (2014) and Yariv (2016); however, their calculations can be recovered by our analysis for weak fluxes. Our theory can also be applied in dissolution/precipitation and desorption/adsorption processes where the boundary conditions of solute fluxes can be approximated as constant, which lays the foundation of understanding the collective autophoretic behaviour in chemically active and ionic many-particle systems (e.g. Papavassiliou & Alexander 2015; Varma, Montenegro-Johnson & Michelin 2018; Rallabandi, Yang & Stone 2019).

Acknowledgements

We thank the NSF CCI-1740630 for support. We thank A. Balazs, T. Emrick and A. Sen for helpful discussions. E. Yariv is thanked for feedback following a talk by F.Y. at the 2017 APS-DFD meeting.

Appendix A. Remarks on the slip velocity in autophoresis with surface solute fluxes

In this appendix, we derive the slip velocity for ionic autophoresis at the outer edge of a two-dimensional (planar) electric double layer (EDL) similar to the analysis in §2.1 of Prieve *et al.* (1984) by changing the zero-flux boundary condition at $y=0$ to

$$\mathbf{j}_{\pm} = -D_{\pm} \left(\nabla c_{\pm} \pm \frac{ze c_{\pm}}{k_B T} \nabla \phi \right), \quad (\text{A } 1a)$$

$$\mathbf{j} = \mathbf{j}_+ \cdot \mathbf{e}_y = -\mathbf{j}_- \cdot \mathbf{e}_y, \quad (\text{A } 1b)$$

$$0 = \mathbf{j}_+ \cdot \mathbf{e}_x = \mathbf{j}_- \cdot \mathbf{e}_x. \quad (\text{A } 1c)$$

At steady state, the conservation of ions requires that

$$\nabla \cdot \mathbf{j}_{\pm} = 0. \quad (\text{A } 2)$$

Since $\partial/\partial y \gg \partial/\partial x$ within the EDL, the leading order of (A 2) is $\partial j_{\pm}/\partial y = 0$, which shows that the normal component of ion fluxes remains constant throughout the EDL. By non-dimensionalizing the normal component of (A 1a) with $Y = y/\lambda_D$, $J = aj/c_{\infty}D$, $C_{\pm} = c_{\pm}/c_{\infty}$ and $\Phi = ze\phi/k_B T$, we have

$$\frac{\lambda_D}{a} J = -\frac{D_{\pm}}{D} \left(\frac{\partial C_{\pm}}{\partial Y} \pm \frac{\partial \Phi}{\partial Y} \right). \quad (\text{A } 3)$$

Therefore, when

$$\frac{\lambda_D}{a} J \ll 1, \quad (\text{A } 4)$$

the Boltzmann distribution will not be disturbed by the surface solute flux. Since

$$\lambda_D = \sqrt{\frac{\epsilon k_B T}{2z^2 e^2 c}} \sim \sqrt{\frac{\epsilon k_B T}{2z^2 e^2 c_{\infty} (1+J)}} = \frac{\lambda_{D\infty}}{\sqrt{1+J}}, \quad (\text{A } 5)$$

the criteria (A 4) can be written as

$$\frac{\lambda_{D\infty} J}{a\sqrt{1+J}} \ll 1, \quad (\text{A } 6)$$

which gives an upper limit for J . For a typical system with $\lambda_{D\infty} = 10$ nm and $a = 1$ μm , (A 6) requires $J \ll 10^4$, which is valid in many experiments on self-propelled colloids (Paxton *et al.* 2005; Howse *et al.* 2007; Sen *et al.* 2009; Wang *et al.* 2013; Brown & Poon 2014).

Therefore, when (A 6) holds, the leading order of the concentration field still satisfies the Boltzmann distribution as in § 2.1 of Prieve *et al.* (1984). Similarly, we note that a finite ion flux at $y = 0$ (which satisfies (A 6)) does not affect the leading-order distribution of the electric potential and velocity field within the EDL and the expression of the slip velocity at the outer edge of the EDL reduces to the result by Prieve *et al.* (1984), given in (2.3).

It has been shown that the expression (2.3) is universal for ionic diffusiophoresis for a $z:z$ electrolyte with arbitrary kinetic model on the surface (Rubinstein & Zaltzman 2001; Zaltzman & Rubinstein 2007). The same conclusion for non-ionic autophoresis with non-zero solute flux can be obtained in a similar manner. The curvature effects are considered by Sabass & Seifert (2012) and Sharifi-Mood *et al.* (2013) for non-ionic diffusiophoresis with surface fluxes and they show the same result, i.e. the solute flux does not change the leading-order expression of the slip velocity.

Appendix B. Properties of Legendre polynomials

The properties of Legendre polynomials listed below are used in deriving (6.7) from (6.6), i.e.

$$\frac{2m+1}{2} \int_{-1}^1 P_n(\tau) P_m(\tau) d\tau = \delta_{mn}, \quad (\text{B } 1a)$$

$$\frac{2m+1}{2} \int_{-1}^1 \tau P_n(\tau) P_m(\tau) d\tau = \frac{m+1}{2m+3} \delta_{n,m+1} + \frac{m}{2m-1} \delta_{n,m-1}, \quad (\text{B } 1b)$$

$$\frac{2m+1}{2} \int_{-1}^1 \frac{P_m(\tau) d\tau}{\sqrt{\cosh \xi_0 - \tau}} = \sqrt{2} e^{-(m+1/2)\xi_0}. \quad (\text{B } 1c)$$

Appendix C. Solutions of model problems

The stream function Ψ for both model problems (i) and (ii) in § 3 can be written in bi-spherical coordinates (ξ, τ) as (Stimson & Jeffery 1926; Brenner 1961; Happel & Brenner 1983)

$$\Psi(\xi, \tau) = (\cosh \xi - \tau)^{-3/2} \sum_{n=1}^{\infty} Q_n(\xi) V_n(\tau), \quad (\text{C } 1)$$

where

$$Q_n(\xi) = d_n \sinh(n - \frac{1}{2})\xi + e_n \sinh(n + \frac{3}{2})\xi + p_n \cosh(n - \frac{1}{2})\xi + q_n \cosh(n + \frac{3}{2})\xi \quad (\text{C } 2)$$

and

$$V_n(\tau) = \frac{P_{n-1}(\tau) - P_{n+1}(\tau)}{2n+1}. \quad (\text{C } 3)$$

We use an additional subscript 'a' and 'b' to distinguish the variables for models (i) and (ii), respectively. For model (i), we have (Jeffery 1912; Happel & Brenner 1983)

$$p_{n,a} = q_{n,a} = 0, \quad (\text{C } 4a)$$

$$d_{n,a} = \frac{U'_a n(n+1) \sinh^2 \xi_0}{\sqrt{2}(2n-1)} \frac{2(1 + e^{-(2n+1)\xi_0}) + (2n+1)(e^{2\xi_0} - 1)}{2 \sinh(2n+1)\xi_0 - (2n+1) \sinh 2\xi_0}, \quad (\text{C } 4b)$$

$$e_{n,a} = -\frac{U'_a n(n+1) \sinh^2 \xi_0}{\sqrt{2}(2n+3)} \frac{2(1 + e^{-(2n+1)\xi_0}) + (2n+1)(1 - e^{-2\xi_0})}{2 \sinh(2n+1)\xi_0 - (2n+1) \sinh 2\xi_0}. \quad (\text{C } 4c)$$

The corresponding hydrodynamic force is

$$F_{H,a} = 8\pi U'_a \sinh \xi_0 \sum_{n=1}^{\infty} \frac{n(n+1)}{(2n-1)(2n+3)} \times \left[\frac{4 \cosh^2(n + \frac{1}{2})\xi_0 + (2n+1)^2 \sinh^2 \xi_0}{2 \sinh(2n+1)\xi_0 - (2n+1) \sinh 2\xi_0} - 1 \right]. \quad (\text{C } 5)$$

The coefficients for model problem (ii) are (Brenner 1961)

$$d_{n,b} = e_{n,b} = 0, \quad (\text{C } 6a)$$

$$p_{n,b} = -\frac{U'_b n(n+1) \sinh^2 \xi_0}{\sqrt{2}(2n-1)} \frac{2(1 - e^{-(2n+1)\xi_0}) + (2n+1)(e^{2\xi_0} - 1)}{2 \sinh(2n+1)\xi_0 + (2n+1) \sinh 2\xi_0}, \quad (\text{C } 6b)$$

$$q_{n,b} = \frac{U'_b n(n+1) \sinh^2 \xi_0}{\sqrt{2}(2n+3)} \frac{2(1 - e^{-(2n+1)\xi_0}) + (2n+1)(1 - e^{-2\xi_0})}{2 \sinh(2n+1)\xi_0 + (2n+1) \sinh 2\xi_0}. \quad (\text{C } 6c)$$

The corresponding hydrodynamic force is

$$F_{H,b} = 8\pi U'_b \sinh \xi_0 \sum_{n=1}^{\infty} \frac{n(n+1)}{(2n-1)(2n+3)} \times \left[\frac{4 \sinh^2(n + \frac{1}{2})\xi_0 - (2n+1)^2 \sinh^2 \xi_0}{2 \sinh(2n+1)\xi_0 + (2n+1) \sinh 2\xi_0} - 1 \right]. \quad (\text{C } 7)$$

Finally the vorticity on S_1 is (Rallabandi *et al.* 2017)

$$\Omega'(\xi_0, \tau) = \frac{R(\xi_0, \tau)g(\xi_0, \tau)}{(1 - \tau^2) \sinh^4 \xi_0}, \quad (\text{C } 8)$$

where

$$g(\xi_0, \tau) = (\cosh \xi_0 - \tau)^{5/2} \times \sum_{n=1}^{\infty} \left[V_n(\tau) \left(\frac{d^2 Q_n(\xi_0)}{d\xi^2} - \frac{2 \sinh \xi_0}{\cosh \xi_0 - \tau} \frac{dQ_n(\xi_0)}{d\xi} + \frac{3(\cosh \xi_0 + 3\tau)}{4(\cosh \xi_0 - \tau)} Q_n(\xi_0) \right) + (1 - \tau^2) Q_n(\xi_0) \left(\frac{d^2 V_n(\tau)}{d\tau^2} + \frac{2}{\cosh \xi_0 - \tau} \frac{dV_n(\tau)}{d\tau} \right) \right]. \quad (\text{C } 9)$$

We note that since $F_{H,a}$, $F_{H,b}$ and Ω' are all linear in U'_a or U'_b , the velocities in model problems U'_a and U'_b will cancel out in (6.11).

REFERENCES

- ANDERSON, J. L. 1989 Colloid transport by interfacial forces. *Annu. Rev. Fluid Mech.* **21**, 61–99.
- ANDERSON, J. L., LOWELL, M. E. & PRIEVE, D. C. 1982 Motion of a particle generated by chemical gradients. Part 1. Non-electrolytes. *J. Fluid Mech.* **117**, 107–121.
- BARABAN, L., TASINKEVYCH, M., POPESCU, M. N., SANCHEZ, S., DIETRICH, S. & SCHMIDT, O. G. 2012 Transport of cargo by catalytic Janus micro-motors. *Soft Matt.* **8**, 48–52.
- BAZANT, M. Z., KILIC, M. S., STOREY, B. D. & AJDARI, A. 2009 Towards an understanding of induced-charge electrokinetics at large applied voltages in concentrated solutions. *Adv. Colloid Interface Sci.* **152**, 48–88.
- BIRD, R. B., STEWART, W. E. & LIGHTFOOT, E. N. 1960 *Transport Phenomena*. Wiley.
- BRADY, J. F. 2011 Particle motion driven by solute gradients with application to autonomous motion: continuum and colloidal perspectives. *J. Fluid Mech.* **667**, 216–259.
- BRENNER, H. 1961 The slow motion of a sphere through a viscous fluid towards a plane surface. *Chem. Engng Sci.* **16** (3), 242–251.
- BROWN, A. & POON, W. 2014 Ionic effects in self-propelled Pt-coated Janus swimmers. *Soft Matt.* **10**, 4016–4027.
- CÓRDOVA-FIGUEROA, U. M. & BRADY, J. F. 2008 Osmotic propulsion: the osmotic motor. *Phys. Rev. Lett.* **100**, 158303.
- DASH, S., MURTH, P. N., NATH, L. & CHOWDHURY, P. 2010 Kinetic modeling on drug release from controlled drug delivery systems. *Acta Pol. Pharm.* **67** (3), 217–223.
- DERJAGUIN, B. V., SIDORENKOV, G. P., ZUBASHCHENKOV, E. A. & KISELEVA, E. V. 1947 Kinetic phenomena in boundary films of liquids. *Kolloidn. Z.* **9**, 335–347.
- EBBENS, S., GREGORY, D. A., DUNDERDALE, G., HOWSE, J. R., IBRAHIM, Y., LIVERPOOL, T. B. & GOLESTANIAN, R. 2014 Electrokinetic effects in catalytic platinum-insulator Janus swimmers. *Europhys. Lett.* **106**, 58003.
- FIGLIUZZI, B., CHAN, W. H. R., MORAN, J. L. & BUIE, C. R. 2014 Nonlinear electrophoresis of ideally polarizable particles. *Phys. Fluids* **26**, 102002.
- GOLESTANIAN, R., LIVERPOOL, T. B. & AJDARI, A. 2007 Designing phoretic micro- and nano-swimmers. *New J. Phys.* **9**, 126.
- HAPPEL, J. & BRENNER, H. 1983 *Low Reynolds Number Hydrodynamics*. Martinus Nijhoff Publishers.
- HOWSE, J. R., JONES, R. A. L., RYAN, A. J., GOUGH, T., VAFABAKHSH, R. & GOLESTANIAN, R. 2007 Self-motile colloidal particles: from directed propulsion to random walk. *Phys. Rev. Lett.* **99**, 048102.
- IBRAHIM, Y., GOLESTANIAN, R. & LIVERPOOL, T. B. 2017 Multiple phoretic mechanisms in the self-propulsion of a Pt-insulator Janus swimmer. *J. Fluid Mech.* **828**, 318–352.
- ISRAELACHVILI, J. 2011 *Intermolecular and Surface Forces*, 3rd edn. Academic Press.
- IZRI, Z., VAN DER LINDEN, M. N., MICHELIN, S. & DAUCHOT, O. 2014 Self-propulsion of pure water droplets by spontaneous Marangoni-stress-driven motion. *Phys. Rev. Lett.* **113**, 248302.
- JEFFERY, G. B. 1912 On a form of the solution of Laplace's equation suitable for problems relating to two spheres. *Proc. R. Soc. Lond. A* **87** (593), 109–120.
- JOHNSON, K. A. & GOODY, R. S. 2011 The original Michaelis constant: translation of the 1913 Michaelis–Menten paper. *Biochem.* **50**, 8264–8269.
- KILIC, M. S., BAZANT, M. Z. & AJDARI, A. 2007 Steric effects in the dynamics of electrolytes at large applied voltages. I. Double-layer charging. *Phys. Rev. E* **75**, 021502.
- LEAL, L. G. 2007 *Advanced Transport Phenomena: Fluid Mechanics and Convective Transport Processes*. Cambridge University Press.
- MANCINELLI, R., BOTTI, A., BRUNI, F., RICCI, M. A. & SOPER, A. K. 2007 Hydration of sodium, potassium, and chloride ions in solution and the concept of structure maker/breaker. *J. Phys. Chem. B* **111**, 13570–13577.
- MICHAELIS, L. & MENTEN, M. L. 1913 Die kinetik der invertinwirkung. *Biochem. Z.* **49**, 333–369.
- MICHELIN, S. & LAUGA, E. 2014 Phoretic self-propulsion at finite Peclet numbers. *J. Fluid Mech.* **747**, 572–604.
- MICHELIN, S. & LAUGA, E. 2015 Autophoretic locomotion from geometric asymmetry. *Eur. Phys. J. E* **38**, 7.

- MICHELIN, S., LAUGA, E. & BARTOLO, D. 2013 Spontaneous autophoretic motion of isotropic particles. *Phys. Fluids* **25**, 061701.
- MOERMAN, P. G., MOYSES, H. W., VAN DER WEE, E. B., GRIER, D. G., VAN BLAADEREN, A., KEGEL, W. K., GROENEWOLD, J. & BRUJIC, J. 2017 Solute-mediated interactions between active droplets. *Phys. Rev. E* **96**, 032607.
- MORAN, J. L. & POSNER, J. D. 2011 Electrokinetic locomotion due to reaction-induced charge auto-electrophoresis. *J. Fluid Mech.* **680**, 31–66.
- MORAN, J. L. & POSNER, J. D. 2014 Role of solution conductivity in reaction induced charge auto-electrophoresis. *Phys. Fluids* **26**, 042001.
- MORAN, J. L. & POSNER, J. D. 2017 Phoretic self-propulsion. *Annu. Rev. Fluid Mech.* **49**, 511–540.
- MOZAFFARI, A., SHARIFI-MOOD, N., KOPLIK, J. & MALDARELLI, C. 2016 Self-diffusiophoretic colloidal propulsion near a solid boundary. *Phys. Fluids* **28**, 053107.
- PALACCI, J., ABÉCASSIS, B., COTTIN-BIZONNE, C., YBERT, C. & BOCQUET, L. 2010 Colloidal motility and pattern formation under rectified diffusiophoresis. *Phys. Rev. Lett.* **104**, 138302.
- PAPAVASSILIOU, D. & ALEXANDER, G. P. 2015 The many-body reciprocal theorem and swimmer hydrodynamics. *Europhys. Lett.* **110**, 44001.
- PAXTON, W. F., BAKER, P. T., KLINE, T. R., WANG, Y., MALLOUK, T. E. & SEN, A. 2006 Catalytically induced electrokinetics for motors and micropumps. *J. Am. Chem. Soc.* **128**, 14881–14888.
- PAXTON, W. F., SEN, A. & MALLOUK, T. E. 2005 Motility of catalytic nanoparticles through self-generated forces. *Chem. Eur. J.* **11**, 6462–6470.
- PRIEVE, D. C., ANDERSON, J. L., EBEL, J. P. & LOWELL, M. E. 1984 Motion of a particle generated by chemical gradients. Part 2. Electrolytes. *J. Fluid Mech.* **148**, 247–269.
- RALLABANDI, B., HILGENFELDT, S. & STONE, H. A. 2017 Hydrodynamic force on a sphere normal to an obstacle due to non-uniform flow. *J. Fluid Mech.* **818**, 407–434.
- RALLABANDI, B., YANG, F. & STONE, H. A. 2019 Motion of hydrodynamically interacting active particles. [arXiv:1901.04311](https://arxiv.org/abs/1901.04311).
- RUBINSTEIN, I. & ZALTZMAN, B. 2001 Electro-osmotic slip of the second kind and instability in concentration polarization at electro dialysis membranes. *Math. Models Meth. Appl. Sci.* **11** (2), 263–300.
- SABASS, B. & SEIFERT, U. 2012 Dynamics and efficiency of a self-propelled, diffusiophoretic swimmer. *J. Chem. Phys.* **136**, 064508.
- SAFDAR, M., KHAN, S. U. & JÄNIS, J. 2018 Progress toward catalytic micro- and nanomotors for biomedical and environmental applications. *Adv. Mater.* **30**, 1703660.
- SCHNITZER, O. & YARIV, E. 2015 Osmotic self-propulsion of slender particles. *Phys. Fluids* **27**, 031701.
- SEN, A., IBELE, M., HONG, Y. & VELEGOL, D. 2009 Chemo- and phototactic nano/microbots. *Faraday Discuss.* **143**, 15–27.
- SHARIFI-MOOD, N., KOPLIK, J. & MALDARELLI, C. 2013 Diffusiophoretic self-propulsion of colloids driven by a surface reaction: the submicron particle regime for exponential and van der Waals interactions. *Phys. Fluids* **25**, 012001.
- SHIN, S., UM, E., SABASS, B., AULT, J. T., RAHIMI, M., WARREN, P. B. & STONE, H. A. 2016 Size-dependent control of colloid transport via solute gradients in dead-end channels. *Proc. Natl Acad. Sci. USA* **113** (2), 257–261.
- SHKLYAEV, S., BRADY, J. F. & CÓRDOVA-FIGUEROA, U. M. 2014 Non-spherical osmotic motor: chemical sailing. *J. Fluid Mech.* **748**, 488–520.
- STIMSON, M. & JEFFERY, G. B. 1926 The motion of two spheres in a viscous fluid. *Proc. R. Soc. Lond. A* **111** (757), 110–116.
- STONE, H. A. & SAMUEL, A. D. T. 1996 Propulsion of microorganisms by surface distortions. *Phys. Rev. Lett.* **77** (19), 4102–4104.
- TÁTULEA-CODREAN, M. & LAUGA, E. 2018 Artificial chemotaxis of phoretic swimmers: instantaneous and long-time behaviour. *J. Fluid Mech.* **856**, 921–957.
- VARMA, A., MONTENEGRO-JOHNSON, T. D. & MICHELIN, S. 2018 Clustering-induced self-propulsion of isotropic autophoretic particles. *Soft Matt.* **14**, 7155–7173.

- VELEGOL, D., GARG, A., GUHA, R., KAR, A. & KUMAR, M. 2016 Origins of concentration gradients for diffusiophoresis. *Soft Matt.* **12** (21), 4686–4703.
- WANG, W., CHIANG, T., VELEGOL, D. & MALLOUK, T. E. 2013 Understanding the efficiency of autonomous nano- and microscale motors. *J. Am. Chem. Soc.* **135**, 10557–10565.
- YARIV, E. 2011 Electrokinetic self-propulsion by inhomogeneous surface kinetics. *Proc. R. Soc. Lond. A* **467**, 1645–1664.
- YARIV, E. 2016 Wall-induced self-diffusiophoresis of active isotropic colloids. *Phys. Rev. Fluids.* **1**, 032101.
- ZALTZMAN, B. & RUBINSTEIN, I. 2007 Electro-osmotic slip and electroconvective instability. *J. Fluid Mech.* **579**, 173–226.